

## Electric-Field Control of Solitons in a Ferroelectric Organic Charge-Transfer Salt

F. Kagawa,<sup>1,2</sup> S. Horiuchi,<sup>3</sup> H. Matsui,<sup>3,4</sup> R. Kumai,<sup>3</sup> Y. Onose,<sup>1,5</sup> T. Hasegawa,<sup>3</sup> and Y. Tokura<sup>1,5,3,6</sup>

<sup>1</sup>Multiferroics Project, ERATO, Japan Science and Technology Agency (JST), c/o Department of Applied Physics, University of Tokyo, Tokyo 113-8656, Japan

<sup>2</sup>Department of Applied Physics and Quantum-Phase Electronics Center (QPEC), University of Tokyo, Tokyo 113-8656, Japan

<sup>3</sup>National Institute of Advanced Industrial Science and Technology (AIST), Tsukuba 305-8562, Japan

<sup>4</sup>Department of Advanced Materials Science, University of Tokyo, Kashiwa, Chiba 277-8561, Japan

<sup>5</sup>Department of Applied Physics, University of Tokyo, Tokyo 113-8656, Japan

<sup>6</sup>Cross-Correlated Materials Research Group (CMRG) and Correlated Electron Research Group (CERG), ASI-RIKEN, Wako 351-0198, Japan

(Received 11 March 2010; published 2 June 2010)

The role of solitons in transport, dielectric, and magnetic properties has been revealed for the quasi-one-dimensional organic charge-transfer salt, TTF-QBrCl<sub>3</sub> [tetrathiafulvalene (TTF)-2-bromo-3,5,6-trichloro-*p*-benzoquinone (QBrCl<sub>3</sub>)]. The material was found to be ferroelectric and hence the solitons should be located at the boundary of the segments with opposite electric polarization. This feature enabled the electric-field control of soliton density and hence the clear-cut detection of soliton contributions. The gigantic dielectric response in the ferroelectric phase is ascribed to the dynamical bound and creeping motions of spinless solitons.

DOI: 10.1103/PhysRevLett.104.227602

PACS numbers: 77.22.-d, 75.60.Ch, 76.20.+q, 77.84.Jd

Electrons confined to a one-dimensional (1D) chain exhibit rich physics [1]. The lattice-modulated charge-density wave (CDW) is one of the paradigms [2]. Although the CDW ground state is classified as a band insulator, its low-energy excitations are collective modes, i.e., “wavelike” phasons and amplitudons [3]. This situation becomes more intriguing when the lattice modulation is dimerization with degenerate patterns; here, the phason mode vanishes but “particlelike” solitons (or “misfits” in dimerization) appear as low-energy excitations instead [4,5]. In *trans*-polyacetylene, the systematic control of soliton density by chemical doping has revealed that solitons are largely responsible for the charge transport and magnetic properties [6], yet a high degree of structural disorder of the polymers has made conclusive arguments of soliton dynamics challenging. The dimerized organic charge-transfer (CT) salts are another candidate in which solitons may play a major role [7–14]. However, the soliton density has never been controlled in the organic CT salts, and therefore the role of solitons, especially in transport and dielectric properties, has remained far from thorough understanding. In this Letter, we reveal the soliton contributions to various physical properties in the dimerized organic CT salt, TTF-QBrCl<sub>3</sub>. By exploiting the ferroelectricity coupled to the dimerization pattern, we could control the soliton density by using an electric field. This unique method has enabled us to extract the soliton contribution directly.

TTF-QBrCl<sub>3</sub> has a quasi-1D structure composed of mixed stacks of  $\pi$ -electron donor (*D*; TTF) and acceptor (*A*; QBrCl<sub>3</sub>) molecules [15]. As in the case of the prototypical neutral-to-ionic transition (NIT) system TTF-QCl<sub>4</sub> (TTF-*p*-chloranil) [16], TTF-QBrCl<sub>3</sub> undergoes the first-

order NIT at  $T_c$  ( $\approx 70$  K) but with more enhanced valence fluctuations [12,15]. At high temperatures the system is nominally neutral and the degree of charge transfer  $\rho \sim 0.3$ , while at low temperatures nominally ionic and  $\rho \sim 0.6$ . Importantly, as schematically shown in Figs. 1(a) and 1(b), this NIT is accompanied simultaneously by the *D*-*A* dimerization [15,17] and thus possesses an aspect of Peierls transition. In the ionic phase, the two different dimerization patterns are obviously degenerate [Fig. 1(b)]; hence, the prerequisite for soliton excitation

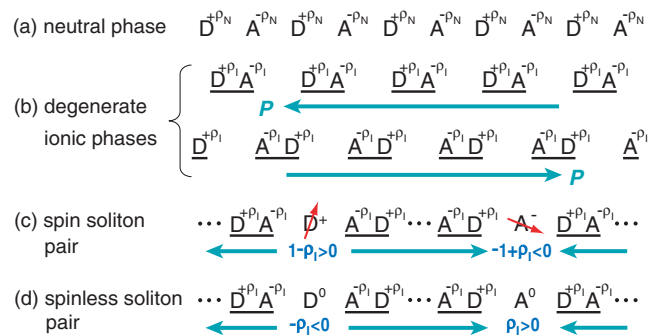


FIG. 1 (color online). Schematic illustrations of mixed stack composed of donor (*D*) and acceptor (*A*) molecules. (a) and (b) Neutral and ionic stacks with charge transfer  $\rho_N$  ( $\sim 0.3$ ) and  $\rho_I$  ( $\sim 0.6$ ), respectively. (c) A pair of spin soliton and spin antisoliton. (d) A pair of spinless soliton and spinless antisoliton. The small and large arrows and underlines represent spin-1/2, electric polarization *P*, and a dimer singlet state, respectively. For simplicity, the chemical structures of solitons are drawn as an abrupt change in the *P* direction in the strong-dimerization limit. In (c) and (d), fractional charge carried by each soliton is also presented in this strong coupling limit.

is satisfied in TTF-QBrCl<sub>3</sub> [4,5,10]. The mechanism of NIT itself has been an intriguing subject [10–12,18–23], but in this Letter we focus on the roles of solitons in macroscopic properties of the dimerized ionic phase.

The soliton excitation includes two types: spin soliton [Fig. 1(c)] and spinless soliton [Fig. 1(d)]. The two solitons both carry fractional charges but the signs are opposite [Figs. 1(c) and 1(d); see also Ref. [5]]. Each soliton should be created or annihilated in pairs: one is centered at  $D$  (=TTF), while the other is at  $A$  (=QBrCl<sub>3</sub>) (say, anti-soliton). As seen below, spinless and spin solitons emergent from the polar crystal structure is a peculiar aspect of TTF-QBrCl<sub>3</sub> and related compounds.

In the ionic phase, the broken symmetry (nonpolar  $P12_1/n1 \rightarrow$  polar  $P1n1$ ; Ref. [15]) via the  $D$ - $A$  dimerization results in electric polarization coupled to the dimerization pattern [Fig. 1(b)]. We observed the spontaneous polarization  $P$  along the  $D$ - $A$  stack (the  $a$  axis) [Fig. 2(a)] after the dc electric field ( $E_{dc}$ ) cooling of  $\sim 0.95$  kV/cm; the  $P$  direction can be reversed by changing the sign of the poling electric field, corroborating the ferroelectric nature. The ferroelectric aspect of NIT is also consistent with the strong enhancement of dielectric constant  $\epsilon_1$  ( $\parallel a$ ) around  $T_c$  [Fig. 2(b); see also Ref. [15]].

Another salient feature in Fig. 2(b) is the dielectric dispersion in the ionic phase. Note that just below  $T_c$ ,  $\epsilon_1$  at 600 MHz is considerably smaller than  $\epsilon_1$  at 1 kHz. From the dielectric spectra of  $\epsilon_1$  and  $\epsilon_2$  (the imaginary part), we found that this dispersive nature is associated with relaxa-

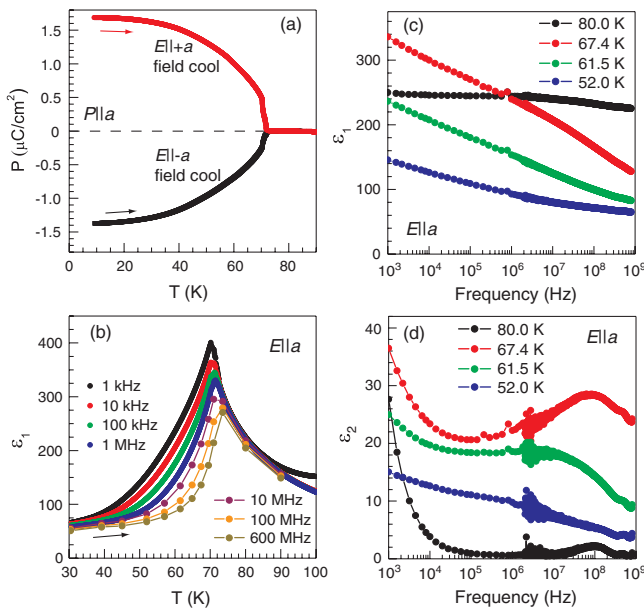


FIG. 2 (color online). (a),(b) Temperature dependence of spontaneous polarization (a) and dielectric constant at various frequencies (b) along the mixed stack (the  $a$  axis). The polarization was obtained from the pyroelectric current. (c),(d) Dielectric spectra of  $\epsilon_1$  (c) and  $\epsilon_2$  (d) from 1 kHz to 800 MHz. Here,  $\epsilon_1$  was measured by using a LCR meter below 2 MHz and an impedance analyzer above that.

tion behavior; in Figs. 2(c) and 2(d), the polydispersive relaxation-type spectra are appreciable only below  $T_c$  with characteristic frequencies of  $\sim 100$  MHz for 67.4 K and  $\sim 10$  MHz for 61.5 K. Such MHz dynamics of the dielectric relaxation seems too slow to be ascribed to the (diffusive) soft phonon mode (typically sub-THz region; see Refs. [12,24]) but too fast to the mobile ferroelectric two-dimensional domain-wall sheet. The most plausible origin is the pinned boundary motion of 1D ferroelectric segments with opposite  $P$ , that is, local oscillation of solitons within the stack. Note that x-ray diffuse scattering measurements in the closely related compound TTF-QCl<sub>4</sub> revealed highly 1D nature of structural fluctuations [25]; therefore the pinned soliton motions in the neighboring stacks are also expected nearly independent. The frequency ( $\omega$ ) dependent nature of  $\epsilon_1$  peak temperature [Fig. 2(b)] also implies that the  $\epsilon_1$  enhancement is partially related to some spatially inhomogeneous dynamics such as the soliton motion; in the case just near  $T_c$ , the motion of boundaries between neutral and ionic segments likely contributes to  $\epsilon_1$  as well [10]. These inhomogeneous states may be favored by local field randomness due to the orientational disorder of Br position in a QBrCl<sub>3</sub> molecule.

To settle longstanding arguments on the possible roles of solitons [11,12,14], more persuasive evidences are needed, such as the direct detection of soliton contribution via the control of soliton density. In this context, the observation of spontaneous  $P$  [Fig. 2(a)] incorporates a valuable implication; the single-domain or less-multi-domain state can be prepared by the poling procedure. Since in TTF-QBrCl<sub>3</sub> the soliton can be viewed as a boundary between the dimerized ferroelectric segments, the less-multi domain state after the poling should correspond to a “soliton-poor” state. This electric-field control of soliton density is applicable *in situ* without changing the influence of disorder. Thus, we can address straightforwardly how the solitons affect various physical properties by comparing the before-poling state (“BP”) with the after-poling state (“AP”). Below we show the soliton contributions to the dielectric, dc transport, and magnetic properties in sequence.

The change in  $\epsilon_1(T)$  due to the poling is demonstrated in Fig. 3(a), where  $\epsilon_1$  at 1 kHz and the dielectric dispersion in the ionic phase are both dramatically diminished. As mentioned above, the difference between the BP (soliton-rich) and AP (soliton-poor) states,  $\Delta\epsilon_1$ , is attributable to the soliton contribution; for clarity,  $\Delta\epsilon_1$  at 1 kHz is presented in Fig. 3(b). This confirms that the pinned relaxational motion of solitons is the origin of the dispersive  $\epsilon_1$  in the dimerized ionic phase. The soliton density is clearly history (BP or AP) dependent [Fig. 3(a)], demonstrating that most of solitons in TTF-QBrCl<sub>3</sub> is not thermally excited but adventitiously generated upon the NIT. At low temperatures,  $\Delta\epsilon_1$  at 1 kHz nearly vanishes [Fig. 3(b)], probably because the solitons becomes “frozen” (i.e., strongly pinned) at least at a frequency window of 1 kHz.

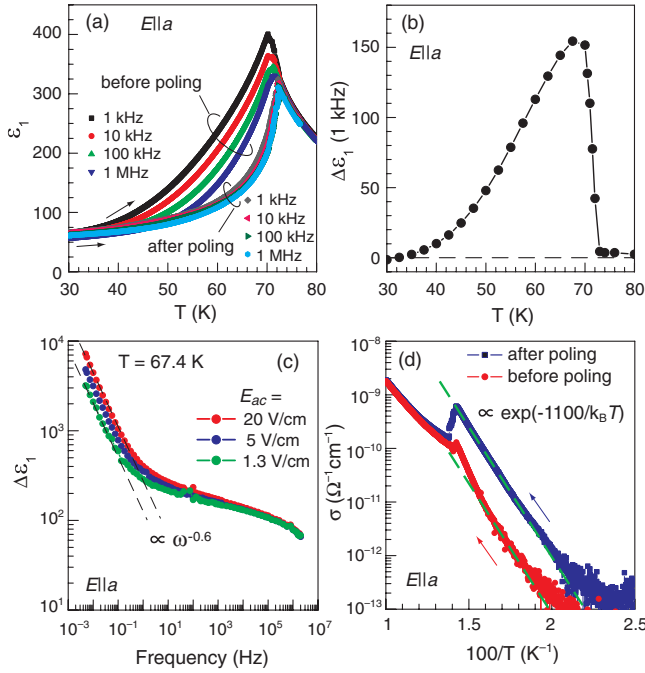


FIG. 3 (color online). (a) Dielectric dispersion ( $\parallel a$ ) before and after the poling procedure of  $\sim 0.95$  kV/cm. (b) Soliton contributions  $\Delta\epsilon_1$  at 1 kHz obtained from (a). (c) Dielectric spectra of solitons under various magnitudes of  $E_{ac}$  at 67.4 K. For the  $\epsilon_1$  below 1 kHz, a Solartron 1260 with a 1296 dielectric interface was used. (d) Transport properties ( $\parallel a$ ) measured under 50 V/cm. The broken lines in (c) and (d) stand for  $\omega^{-0.6}$  dependence and Arrhenius law,  $\propto \exp(-1100/k_B T)$ , respectively. The data in (a) and (d) were taken with increasing temperature.

Naturally, the pinned relaxational motion turns into the depinned creep motion under strong, low- $\omega$  ac electric fields ( $E_{ac}$ ). In the low- $\omega$  region just below  $T_c$ , we found that the  $\epsilon_1$  spectra of soliton contributions shows  $\omega^{-\beta}$  dependence with  $\beta \approx 0.6-0.7$ ; for example, that occurs in the mHz region at 67.4 K [Fig. 3(c)]. Moreover, in this regime,  $\Delta\epsilon_1$  depends markedly on the magnitude of  $E_{ac}$ . The observed  $0 < \beta < 1$  behavior together with nonlinear (i.e.,  $E_{ac}$  dependent)  $\epsilon_1$  is known as an indication of the creep motion [26,27]; thus the mHz-region dynamics in Fig. 3(c) is attributable to the creep motion of solitons. In such slow dynamics, interstack interaction of solitons may play some role; it should be noted that the interstack correlation is relevant at least to the three-dimensional static order, as manifested in a jump in lattice constant normal to the stack at NIT [15].

In the dc transport properties, solitons are also anticipated to play a major role. In *trans*-polyacetylene, dc conductivity  $\sigma$  largely increases with soliton density and, at least at the low doping levels, the  $\sigma$  is thought to be associated with the soliton motion [6]. The natural question arising here is whether the creeping solitons are responsible for the dc transport in TTF-QBrCl<sub>3</sub>. Figure 3(d) shows the temperature profile of  $\sigma$  with the different density of soliton. Remarkably, in the present case it is

the soliton-poor (AP) state that exhibits higher  $\sigma$ . The difference of  $\sigma$  between BP and AP is gigantic and amounts to nearly 1 order of magnitude. Nevertheless the two  $\sigma(T)$  curves in the ionic phase are roughly approximated by the Arrhenius law,  $\propto \exp(-\Delta/k_B T)$ , with the nearly identical  $\Delta$  of  $\sim 1100$  K. Thus, we conclude that in TTF-QBrCl<sub>3</sub> under weak  $E_{dc}$ , the creeping soliton is not the primal charge carrier but rather the carrier scatterer. The estimated  $\Delta$  is much smaller than the optical CT gap of  $\sim 7200$  K [28]; this fact may indicate that the thermally excited carrier is polaron or its analog whose mean free path is dominated by the density of charged solitons.

Up to now, we have not been able to identify which soliton—spin-carrying or spinless—is relevant to  $\epsilon_1$  and  $\sigma$ , because in principle both solitons can affect them. However, ESR can detect only spin solitons, thereby being a powerful, spin-nature-specific measurement. We carried out a X-band ESR measurement, combined with the electric-field-application setup. The magnetic field  $H$  was applied along the direction in the  $ac$  plane with the angle of  $20^\circ$  from the  $a$  axis, since the two-line nature of ESR spectra, i.e., soliton-antisoliton pair, is clearly discernible.

The ESR results are shown in Figs. 4(a) and 4(b). As a whole, the profiles of the BP state reproduce well the previous results on TTF-QCl<sub>4</sub> [9]: the two ESR signals with equal integrated intensity arise from the spin solitons located at QBrCl<sub>3</sub> and TTF below  $T_c$  ( $\approx 70$  K in the case of TTF-QBrCl<sub>3</sub>) [Fig. 4(a)]. The temperature dependence of signal intensity is approximated by the Curie law ( $\propto 1/T$ ) [Fig. 4(b)], incorporating the following two implications. First, the spin soliton density is nearly temperature-independent, and therefore most of spin solitons in TTF-QBrCl<sub>3</sub> are adventitious. Second, the spin moments are basically noninteracting; i.e., the spin solitons are mutually well separated. Assuming spin- $\frac{1}{2}$ , we estimated that the density of spin soliton (or antisoliton) is the order of  $10^{-5}$  per TTF (or QBrCl<sub>3</sub>) molecule, even more dilute than the case of TTF-QCl<sub>4</sub> ( $\sim 10^{-4}$ ) [9].

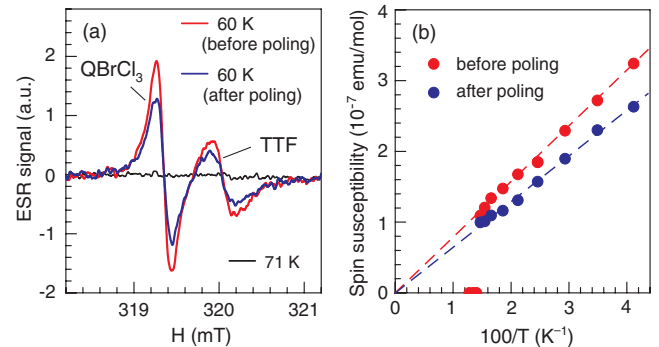


FIG. 4 (color online). ESR signal arising from the spin solitons. (a) Temperature-dependent and poling-procedure-dependent variations in the ESR spectra of TTF-QBrCl<sub>3</sub>. (b) Temperature dependence of ESR signal intensity. An electric field of  $\sim 1$  kV/cm was used for the poling. The broken lines in (b) are the guide for the eyes, representing the Curie law.

The new feature revealed here is that the spin soliton density is suppressed by the poling of  $\sim 1$  kV/cm [Figs. 4(a) and 4(b)]. This observation corroborates that the ESR signal arises from the spin solitons located at the boundary of ferroelectric segments. However, the degree of suppression was found unexpectedly small and only  $\sim 17\%$ . Namely, even in the “soliton-poor” state,  $\sim 83\%$  of the spin solitons are still remaining. It naturally follows that the intrinsic value of spontaneous polarization should be larger than the value observed in Fig. 2(a),  $\sim 1.7 \mu\text{C}/\text{cm}^2$  (in a different piece of the crystal, we found  $\sim 2.1 \mu\text{C}/\text{cm}^2$ ); in fact, the *ab initio* studies predict  $8\text{--}11 \mu\text{C}/\text{cm}^2$  for TTF-QCl<sub>4</sub> [23,29]. Since we confirmed that the stronger poling field of  $\sim 1.3$  kV/cm makes no appreciable difference in the ESR properties, the remaining spin solitons are considered to be pinned strongly enough to least contribute to the polarization current.

Why is the suppression of spin soliton density only  $\sim 17\%$ , even though the most of mobile charge-carrying solitons vanishes as far as seen from  $\epsilon_1$  [Fig. 3(a)]? This subject deserves further investigation but here we put forward a possible scenario that can resolve the apparently conflicting results by considering two kinds of soliton, namely, the spinless and spin solitons. Given that the ESR sees only the spin solitons, we may attribute the mobile solitons captured by dielectric response primarily to the spinless solitons. This hypothesis is consistent with the soliton theory for the NIT system [10]; near  $T_c$ , the spinless soliton likely has a lower excitation energy and its width is expected thicker than the spin solitons. Therefore, the spinless solitons are weakly pinned and relatively easy to be pair-annihilated during the strong  $E_{\text{dc}}$  field cooling, while primarily contributing to  $\epsilon_1$  under  $E_{\text{ac}}$  in the BP state. In contrast, the spin soliton is thinner and subject to the pinning potential. Hence, even under strong  $E_{\text{dc}}$ , the spin solitons are hard to be annihilated, as inferred from the present ESR experiments.

In many of organic donor-acceptor CT salts, the stacking of planar molecules naturally results in a quasi-1D  $\pi$ -electron band and thus possesses Peierls or spin-Peierls instability [30,31]. This implies that the solitons as the boundaries of 1D ferroelectric segment could be ubiquitous in this class of materials. The organic CT salts combined with the electrical control of soliton density may provide a new field for the study of soliton dynamics.

To conclude, we revealed the roles of solitons in various physical properties in the dimerized ionic phase of TTF-QBrCl<sub>3</sub>. By exploiting ferroelectric nature inherent in this system, we found that the density of spinless charged solitons can be controlled to a nearly full extent by an electric-field cooling, while that of spin solitons to a less extent. Through this new control method, it turned out that the spinless solitons critically enhance the dielectric response but suppress the dc conductivity. The electrical control of soliton density provides a new approach to the soliton study in various organic CT salts.

The authors thank N. Nagaosa, T. Arima, N. Furukawa, M. Mochizuki and S. Ishibashi for fruitful discussion. This work was partially supported by Grants-in-Aid for Scientific Researches on Innovative Area (No. 20110003) from the MEXT and for Scientific Research (No. 20340086) from JSPS and by FIRST Program.

- 
- [1] T. Giamarchi, *Chem. Rev.* **104**, 5037 (2004).
  - [2] For a review, see G. Gruner, *Density Waves in Solids* (Addison-Wesley, Reading, MA, 1994).
  - [3] P. A. Lee, T. M. Rice, and P. W. Anderson, *Solid State Commun.* **14**, 703 (1974).
  - [4] W. P. Su, J. R. Schrieffer, and A. J. Heeger, *Phys. Rev. Lett.* **42**, 1698 (1979).
  - [5] M. J. Rice and E. J. Mele, *Phys. Rev. Lett.* **49**, 1455 (1982).
  - [6] For a review, see A. J. Heeger, S. Kivelson, J. R. Schrieffer, and W.-P. Su, *Rev. Mod. Phys.* **60**, 781 (1988).
  - [7] R. C. Hughes and Z. G. Soos, *J. Chem. Phys.* **48**, 1066 (1968).
  - [8] B. M. Hoffman and R. C. Hughes, *J. Chem. Phys.* **52**, 4011 (1970).
  - [9] T. Mitani, G. Saito, Y. Tokura, and T. Koda, *Phys. Rev. Lett.* **53**, 842 (1984).
  - [10] N. Nagaosa, *J. Phys. Soc. Jpn.* **55**, 2754 (1986).
  - [11] H. Okamoto *et al.*, *Phys. Rev. B* **43**, 8224 (1991).
  - [12] Y. Okimoto, S. Horiuchi, E. Saitoh, R. Kumai, and Y. Tokura, *Phys. Rev. Lett.* **87**, 187401 (2001).
  - [13] S. A. Bewick and Z. G. Soos, *Chem. Phys.* **325**, 60 (2006).
  - [14] Y. Tokura *et al.*, *Phys. Rev. Lett.* **63**, 2405 (1989).
  - [15] S. Horiuchi, Y. Okimoto, R. Kumai, and Y. Tokura, *J. Phys. Soc. Jpn.* **69**, 1302 (2000).
  - [16] J. B. Torrance *et al.*, *Phys. Rev. Lett.* **47**, 1747 (1981).
  - [17] M. Le Cointe *et al.*, *Phys. Rev. B* **51**, 3374 (1995).
  - [18] T. Iizuka-Sakano and Y. Toyozawa, *J. Phys. Soc. Jpn.* **65**, 671 (1996).
  - [19] Y. Anusooya-Pati, Z. G. Soos, and A. Painelli, *Phys. Rev. B* **63**, 205118 (2001).
  - [20] V. Oison, C. Katan, P. Rabiller, M. Souhassou, and C. Koenig, *Phys. Rev. B* **67**, 035120 (2003).
  - [21] Z. G. Soos, S. A. Bewick, A. Peri, and A. Painelli, *J. Chem. Phys.* **120**, 6712 (2004).
  - [22] Z. G. Soos and A. Painelli, *Phys. Rev. B* **75**, 155119 (2007).
  - [23] G. Giovannetti, S. Kumar, A. Stroppa, J. van den Brink, and S. Picozzi, *Phys. Rev. Lett.* **103**, 266401 (2009).
  - [24] M. Masino, A. Girlando, and Z. G. Soos, *Chem. Phys. Lett.* **369**, 428 (2003).
  - [25] M. Le Cointe *et al.*, *Phys. Rev. Lett.* **96**, 205503 (2006).
  - [26] Th. Braun, W. Kleemann, J. Dec, and P. A. Thomas, *Phys. Rev. Lett.* **94**, 117601 (2005).
  - [27] W. Kleemann, *Annu. Rev. Mater. Res.* **37**, 415 (2007).
  - [28] C. S. Jacobsen and J. B. Torrance, *J. Chem. Phys.* **78**, 112 (1983).
  - [29] S. Ishibashi and K. Terakura [Physica B (Amsterdam) (to be published)].
  - [30] J. B. Torrance, *Acc. Chem. Res.* **12**, 79 (1979).
  - [31] F. Kagawa *et al.*, *Nature Phys.* **6**, 169 (2010).